

Dynamical density correlation function of 1D Mott insulators in a magnetic field

Davide Controzzi^(a,b) and Fabian H.L. Essler^(c)

^(a) *Department of Physics, Princeton University, Princeton NJ08544, USA*

^(b) *International School for Advanced Studies, Trieste 34014, Italy*

^(c) *Department of Physics, Brookhaven National Laboratory, Upton, NY 11973-5000, USA*

We consider the one dimensional (1D) extended Hubbard model at half filling in the presence of a magnetic field. Using field theory techniques we calculate the dynamical density-density correlation function $\chi_{nn}(\omega, q)$ in the low-energy limit. When excitons are formed, a singularity appears in $\chi_{nn}(\omega, q)$ at a particular energy and momentum transfer.

I. INTRODUCTION

Quasi 1D Mott insulators¹ display unusual phenomena like spin-charge separation and dynamical generation of a spectral gap and have therefore attracted much attention in recent years. At present the best realizations of 1D Mott insulators are found in anisotropic antiferromagnets like SrCuO₂ or Sr₂CuO₃. The dynamics of the latter compound has been studied both by angular-resolved photoemission² and by electron energy-loss spectroscopy (EELS)³. EELS measures the dynamical density-density correlation function. Theoretical descriptions of 1D itinerant antiferromagnets are based on the half-filled Hubbard model with a large on-site repulsion U (compared to the hopping matrix element t), which ensures that the single-particle Mott gap is large. In the case of Sr₂CuO₃ it is believed that $U \approx 8t$ and that density-density interactions between neighboring sites need to be taken into account^{2,3}. Given that U is “much” larger than t , strong-coupling expansions around $U = \infty$ are an appropriate starting point. They have been used to determine dynamical correlation functions^{4,5} and to successfully model the EELS data for SrCuO₂³.

There exist other materials believed to be quasi-1D Mott insulators (e.g. the Bechgaard salts⁶), in which the Mott gap is small compared to t . The “weak-coupling” regime $U \lesssim 2t$ in which the Mott gap becomes small is manifestly beyond the range of applicability of strong-coupling expansions. The very existence of a gap precludes the application of conformal field theory^{8,9}. However, this regime is accessible by an approach based on exact field theory methods^{10,11}. In Refs 12,13,14,15 this method has been used to determine the optical conductivity and the single-particle Green’s function for 1D Mott insulators in the weak-coupling regime. Here we employ this approach to calculate the dynamical density-density correlation function. Motivated by suggestions that a magnetic field may generate X-ray edge like threshold singularities¹⁶ in the density-density response, we take into consideration the effects of a magnetic field. The outline of this paper is as follows: in section II we present the field theory description for the low energy degrees of freedom. In section III we determine the dynamical density-density correlation function $\chi_{nn}(\omega, q)$. In section IV we consider an extended Hubbard model with sufficiently strong nearest and next-nearest neighbor

density-density interactions. Here excitons are formed and we determine their contributions to $\chi_{nn}(\omega, q)$. We summarize our results in section V.

II. FIELD THEORY DESCRIPTION

The extended Hubbard model in a magnetic field is described by the Hamiltonian

$$H = -t \sum_{l;\sigma} \left(c_{l,\sigma}^\dagger c_{l+1,\sigma} + \text{h.c.} \right) + U \sum_l n_{l,\uparrow} n_{l,\downarrow} + \sum_{j=1}^2 V_j \sum_l n_l n_{l+j} - \frac{h}{2} \sum_l (n_{l,\uparrow} - n_{l,\downarrow}), \quad (1)$$

where $c_{l,\sigma}$ are fermionic annihilation operators of spin \uparrow ($\sigma = 1$) and \downarrow ($\sigma = -1$), $n_{l,\sigma} = c_{l,\sigma}^\dagger c_{l,\sigma}$ and $n_l = n_{l,\uparrow} + n_{l,\downarrow}$. For $h = 0$ the ground state has spin projection $S^z = 0$ whereas for very large fields $h > h_c$ it is fully polarized. We constrain our analysis to the case where the ground state is partially magnetized, which corresponds to fields $0 \leq h < h_c$. A description of the low-energy degrees of freedom of (1) for weak interactions $0 < 2V_2 < 2V_1 < U \ll t$ is then obtained by standard techniques¹⁷. In the presence of the field h there are four Fermi points $\pm k_{F,\sigma}$ with $k_{F,\downarrow} + k_{F,\uparrow} = \pi/a_0$, where a_0 is the lattice spacing. Taking into account only modes in the vicinity of $k_{F,\sigma}$ we expand

$$c_{l,\sigma} \longrightarrow \sqrt{a_0} \left[e^{ik_{F,\sigma}x} R_\sigma(x) + e^{-ik_{F,\sigma}x} L_\sigma(x) \right], \quad (2)$$

where $x = la_0$. The resulting fermionic field theory can be bosonized with the result

$$\mathcal{L}_s = \frac{1}{16\pi} \left[v_s (\partial_x \Phi_s)^2 - \frac{1}{v_s} (\partial_t \Phi_s)^2 \right], \quad (3)$$

$$\mathcal{L}_c = \frac{1}{16\pi} \left[v_c (\partial_x \Phi_c)^2 - \frac{1}{v_c} (\partial_t \Phi_c)^2 \right] - \lambda \cos(\beta_c \Phi_c). \quad (4)$$

The spin sector is a free bosonic theory whereas the charge sector is described by the integrable Sine-Gordon model (SGM)⁷. Fermionic operators are expressed in terms of the canonical charge and spin bose fields $\Phi_{c,s}$ and their respective dual fields

$$\Theta_{c,s}(t, x) = \frac{-1}{v_{c,s}} \int_{-x}^x dy \partial_t \Phi_{c,s}(t, y) \quad (5)$$

by

$$\begin{aligned} L_\sigma &= \eta_\sigma e^{\frac{i}{4}(\beta_c \Phi_c - \frac{1}{\beta_c} \Theta_c)} e^{\frac{i}{4}\sigma(\beta_s \Phi_s - \frac{1}{\beta_s} \Theta_s)}, \\ R_\sigma &= \eta_\sigma e^{-\frac{i}{4}(\beta_c \Phi_c + \frac{1}{\beta_c} \Theta_c)} e^{-\frac{i}{4}\sigma(\beta_s \Phi_s + \frac{1}{\beta_s} \Theta_s)}. \end{aligned} \quad (6)$$

Here $\eta_\sigma = \eta_\sigma^\dagger$ are Klein factors that fulfill $\{\eta_\sigma, \eta_\tau\} = 2\delta_{\sigma,\tau}$. The spin and charge velocities $v_{c,s}$ and the parameters $\beta_{c,s}$ depend on t, h, U and V .

A. Hubbard model ($V_{1,2} = 0$)

For the Hubbard model $\beta_{c,s}$ and $v_{c,s}$ can be calculated exactly from the Bethe Ansatz solution. The “ η -pairing” $SU(2)$ symmetry of the half-filled Hubbard model¹⁸ fixes $\beta_c = 1$, whereas $\beta_s(h, U)$ is obtained from the solution of a linear integral equation^{8,19}

$$\begin{aligned} \beta_s &= \sqrt{2}Z(\Lambda), \\ Z(\lambda) &= 1 + \int_{-\Lambda}^{\Lambda} d\mu a_2(\lambda - \mu) Z(\mu), \end{aligned} \quad (7)$$

where $2\pi a_2(x) = U[x^2 + U^2/4]^{-1}$. The integration boundary Λ is determined by the condition $\epsilon(\Lambda) = 0$, where

$$\begin{aligned} \epsilon(\lambda) &= h - 4\text{Re}\sqrt{1 - (\lambda - iU/4)^2} + U \\ &+ \int_{-\Lambda}^{\Lambda} d\mu a_2(\lambda - \mu) \epsilon(\mu). \end{aligned} \quad (8)$$

In the limit $U/h \rightarrow 0$ β_s can be calculated analytically

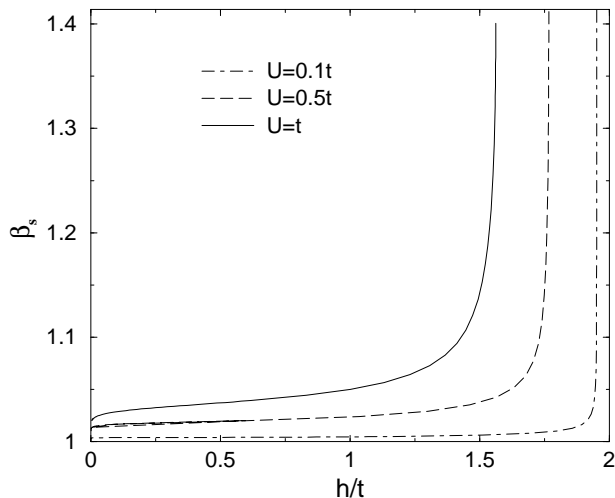


FIG. 1: β_s for the Hubbard model as a function of h for different values of U .

by means of a Wiener-Hopf analysis

$$\beta_s \simeq 1 + \frac{U}{16\pi t \cos(\pi\mathcal{M})}, \quad (9)$$

where \mathcal{M} is the magnetization that is calculated from the solution to an integral equation similar to (8) (see Ref. 8). We note that β_s varies between 1 for $h = 0$ and $\sqrt{2}$ for $h \rightarrow h_c$. The behavior of β_s as a function of h for different values of U is shown in Fig.1. We see that for small values of U β_s remains very close to 1 up to large fields very close to h_c .

The spin and charge velocities can be calculated in a similar way. Field theory is exact in the *scaling limit*, which has been constructed in the absence of a magnetic field in Ref.20 using exact results for the half-filled Hubbard model²¹. The $h > 0$ case can be mapped onto the attractive Hubbard model below half-filling by means of the particle-hole transformation for spin down $c_{j,-1} \rightarrow (-1)^j c_{j,-1}^\dagger$. The scaling limit for the latter model has been found by Woynarovich and Forgacs²² and is obtained by taking $t \rightarrow \infty, U \rightarrow 0$ while keeping

$$\sqrt{Ut \cos^3(\pi\mathcal{M})} e^{-\pi t \cos(\pi\mathcal{M})/2U} = \text{fixed}. \quad (10)$$

In this limit $\beta_s = 1$ and the low-energy effective field theory is $SU(2) \times SU(2)$ symmetric. However, on the level of the large-distance asymptotics of correlation functions of the underlying Hubbard model this enhanced symmetry is broken down to $SU(2) \times U(1)$ by the oscillating factors in (2). For example, the leading asymptotical behavior of the spin-spin correlation functions is

$$\begin{aligned} \langle S^x(x)S^x(0) \rangle &= \langle S^y(x)S^y(0) \rangle = \frac{B(-1)^{x/a_0}}{x} + \dots, \\ \langle S^z(x)S^z(0) \rangle &= \frac{A \cos 2k_{F,\sigma} x}{x} + \dots, \end{aligned} \quad (11)$$

and the spin- $SU(2)$ symmetry is broken. Previous experience^{12,14} suggests that field theory gives a good description of the lattice model in an extended vicinity of the scaling limit, provided the gap is small compared to t . This is the case as long as $U \lesssim 2t$. We will apply field theory in the regime defined by this criterion and therefore allow β_s to be different from 1.

B. Extended Hubbard model

For $V_{1,2} \neq 0$ no exact results for the lattice model (1) are available. However, the low-energy degrees of freedom of (1) in the regime $0 < V_2 < V_1 < \frac{U}{2} \lesssim t$ are still described by (3)-(4), but now with $\beta_c < 1$ ²³. Recently it was shown in Ref.14 that for sufficiently large values of U, V_1, V_2 it is possible to reach the attractive regime of the SGM $\beta_c < 1/\sqrt{2}$, in which excitonic holon-antiholon bound states form. We will first consider the range $1/\sqrt{2} < \beta_c \leq 1$, where no excitons exist and field theory results for the optical conductivity¹³ have been found to be in good agreement with dynamical density matrix renormalization group computations for the lattice model (1)²⁴. In section IV we extend the analysis to the regime $\beta_c < 1/\sqrt{2}$.

C. Density Operator

The density operator is expressed in terms of the spin and charge bosonic fields as¹⁷

$$\begin{aligned} n(x,t) &= n_0(x,t) + \sum_{\sigma} n_{2k_{F,\sigma}}(x,t), \\ n_0(x,t) &= A \partial_x \Phi_c, \\ n_{2k_{F,\sigma}}(x,t) &= A' e^{2ik_{F,\sigma}x} \sin\left(\frac{\beta_c}{2} \Phi_c\right) e^{\frac{i\sigma\beta_s}{2} \Phi_s}. \end{aligned} \quad (12)$$

Here A and A' are numerical constants. For a less than half-filled band there is an additional contribution¹⁷

$$n_U(x,t) = A_U \cos(2[k_{F,\uparrow} + k_{F,\downarrow}]x + \beta_c \Phi_c), \quad (13)$$

which is obtained by integrating out the high-energy degrees of freedom in the path integral representation for the density-density correlation function of the lattice model. The operator (13) corresponds to scattering processes involving two particles and two holes with momentum transfer $2(k_{F,\uparrow} + k_{F,\downarrow}) = 2\pi/a_0$. As a result A_U is proportional to U/t and thus is small. At half-filling we have $A_U = 0$. This can be established by considering the following discrete symmetry of the lattice model

$$c_{j,\sigma} \longleftrightarrow (-1)^j c_{j,-\sigma}^\dagger. \quad (14)$$

The lattice density operator transforms as $n_j \rightarrow 2 - n_j$. In the field theory this symmetry corresponds to inverting the signs of the charge boson and its dual field $\Phi_c \rightarrow -\Phi_c$, $\Theta_c \rightarrow -\Theta_c$. The (normal ordered) density operator $n(x,t)$ must transform to $-n(x,t)$ under this change of sign and this implies that $A_U = 0$.

III. DENSITY CORRELATIONS FOR $\frac{1}{2} < \beta_c^2 \leq 1$

The density-density correlation function is given by

$$G_{nn}(x,t) = G_{nn}^0 + \sum_{\sigma} G_{nn}^{2k_{F,\sigma}}, \quad (15)$$

where

$$\begin{aligned} G_{nn}^0 &= \langle 0 | n_0(x,t) n_0(0,0) | 0 \rangle, \\ G_{nn}^{2k_{F,\sigma}} &= \langle 0 | n_{2k_{F,\sigma}}(x,t) n_{2k_{F,-\sigma}}(0,0) | 0 \rangle. \end{aligned} \quad (16)$$

We note that there are no ‘‘mixed terms’’ as can be shown by exploiting the transformation properties under charge conjugation. Due to spin-charge separation the correlation functions in (16) factorize into spin and charge pieces. In the spin sector (3) we are dealing with a simple Gaussian model and elementary considerations give

$${}_s \langle 0 | e^{i\frac{\beta_s}{2} \Phi_s(x,t)} e^{-i\frac{\beta_s}{2} \Phi_s(0)} | 0 \rangle_s = [x^2 - (v_s t + i\epsilon)^2]^{-d}, \quad (17)$$

where $|0\rangle_s$ denotes the vacuum in the spin sector and

$$d = \beta_s^2/2. \quad (18)$$

In the Hubbard model the exponent d varies between $\frac{1}{2}$ for zero field and 1 for $h \rightarrow h_c$. In order to determine the charge part of the correlators (16) we make use of the integrability of the SGM (4) describing the charge sector. In the range of β_c considered here the spectrum of the SGM consists of scattering states of *solitons* and *antisolitons*, which are particles of mass M , charge $Q = \pm e$ and relativistic dispersion $e(p) = \sqrt{p^2 + M^2}$. In the Hubbard model they correspond to holons and antiholons respectively. It is convenient to parametrize energy and momentum in terms of the rapidity variable θ

$$p = \frac{M}{v_c} \sinh \theta, \quad e = M \cosh \theta. \quad (19)$$

We introduce an index $\varepsilon = \pm$ for solitons and antisolitons. Then a scattering state of n solitons/antisolitons with rapidities $\{\theta_k\}$ and internal indices $\{\varepsilon_k\}$ is denoted by $|\theta_n \dots \theta_1\rangle_{\varepsilon_n, \dots, \varepsilon_1}$. In the spectral representation of this basis of (anti)soliton scattering states we may express the two-point function of an operator \mathcal{O} in the charge sector as

$$\begin{aligned} {}_c \langle 0 | \mathcal{O}(x,t) \mathcal{O}^\dagger(0) | 0 \rangle_c &= \sum_{n=0}^{\infty} \sum_{\varepsilon_i} \int \frac{d\theta_1 \dots d\theta_n}{(2\pi)^n n!} \\ &\times \exp\left[i \sum_{j=1}^n e_j t - p_j x\right] |{}_c \langle 0 | \mathcal{O}(0) | \theta_n \dots \theta_1 \rangle_{\varepsilon_n \dots \varepsilon_1}|^2. \end{aligned} \quad (20)$$

Here p_j and e_j are given by (19), and the form factors ${}_c \langle 0 | \mathcal{O}(0) | \theta_n \dots \theta_1 \rangle_{\varepsilon_n \dots \varepsilon_1}$ can be calculated by exploiting the integrability of the SGM^{10,11}. As a consequence of the transformation properties under charge conjugation of the operators appearing in (15), only intermediate states with an even number of particles will contribute to (20). In order to obtain an accurate result for the large-distance asymptotics it is sufficient to take into account intermediate states with only a small number of particles in the spectral sum (20)²⁵. For the case at hand we have^{10,11}

$$|{}_c \langle 0 | \partial_x \phi_c | \theta_1, \theta_2 \rangle_{\pm\mp}|^2 = |f(2\theta_-) \sinh \theta_+|^2, \quad (21)$$

$$|{}_c \langle 0 | \sin\left(\frac{\beta_c \Phi_c}{2}\right) | \theta_1, \theta_2 \rangle_{\pm\mp}|^2 = Z_1 |f(2\theta_-)|^2, \quad (22)$$

where $\theta_{\pm} = (\theta_1 \pm \theta_2)/2$, Z_1 is a known constant¹¹ and

$$\begin{aligned} f(\theta) &= \frac{F(\theta)}{\cosh\left(\frac{\theta+i\pi}{2\xi}\right)}, \\ F(\theta) &= \sinh \frac{\theta}{2} \exp\left[\int_0^\infty dk \frac{\sin^2\left(\frac{k}{2}\left[\frac{\theta}{\pi} + i\right]\right) \sinh\left(\frac{1-\xi}{2}k\right)}{k \sinh\left(\frac{\xi k}{2}\right) \cosh\left(\frac{k}{2}\right) \sinh k}\right], \\ \xi &= \frac{\beta_c^2}{1 - \beta_c^2}. \end{aligned} \quad (23)$$

EELS measures the imaginary part of the retarded dynamical density-density correlation function

$$\chi_{nn}(\omega, k) = \text{Im} \left\{ i \int_{-\infty}^{\infty} dx \int_0^{\infty} dt e^{i\omega t - ikx} [G_{nn}(x,t)] \right\}$$

$$-G_{nn}(-x, -t) \Big] \Big\} \quad (24)$$

We evaluate $\chi_{nn}(\omega, k)$ in the vicinity of the low-energy modes at $k = 0, 2k_{F,\sigma}$ by Fourier transforming the large-distance asymptotics of the density-density correlation function. The latter is obtained by carrying out the form factor expansion (20) in the charge sector and multiplying it by the spin-piece (17) in the case of the $2k_{F,\sigma}$ response.

A. Small k behavior

In the vicinity of $k = 0$ the dynamical density response is dominated by the contribution from $G_{nn}^0(x, t)$. This contribution does not involve the spin sector and straightforward calculations give

$$\chi_{nn}(\omega, q) = A^2 8M^2 \frac{(v_c q)^2 |f_0(\theta_0)|^2}{s^3 \sqrt{s^2 - 4M^2}} \Theta(s^2 - 4M^2), \quad (25)$$

with $s^2(\omega, q) = \omega^2 - (v_c q)^2$ and $\theta_0 = 2\text{arccosh}(s/2M)$. Above the threshold at $\omega = \sqrt{v_c^2 q^2 + 4M^2}$, $\chi_{nn}(\omega, q)$ increases from zero in a universal square root fashion. This is due to the momentum dependence of the form factors.

From the Heisenberg equations of motions for the lattice density operator one can derive a relation between χ_{nn} and the optical conductivity $\sigma(\omega)$

$$\text{Re } \sigma(\omega) = \lim_{q \rightarrow 0} \frac{\omega}{q^2} \chi_{nn}(\omega, q). \quad (26)$$

The optical conductivity has been calculated in¹³ and agrees with (26) and (25). We note that a contribution of the type (13) to the density operator would violate the relation (26), which is an independent argument showing that $A_U = 0$ ²⁶.

B. Behavior around $k = 2k_{F,\sigma}$

In the vicinity of $k = 2k_{F,\sigma}$ the dynamical density response is dominated by the contribution from $G_{nn}^{2k_{F,\sigma}}(x, t)$ and involves both the spin and the charge sector. The threshold can be determined by considering the lowest intermediate state that couples to the density operator at $k = 2k_{F,\sigma}$, which is a scattering state of one soliton, one antisoliton and one spinon. The total momentum and energy of this state are

$$\begin{aligned} P &= p + q_1 + q_2, \\ E &= v_s |p| + \sum_{j=1}^2 \sqrt{M^2 + v_c^2 q_j^2}. \end{aligned} \quad (27)$$

The threshold is obtained by minimizing the energy at fixed total momentum with respect to p, q_1, q_2

$$\begin{aligned} E_{\text{thres}} &= \min_{q_1, q_2} \left[v_s |P - q_1 - q_2| + \sum_{j=1}^2 \sqrt{M^2 + v_c^2 q_j^2} \right] \\ &= \begin{cases} \sqrt{4M^2 + v_c^2 P^2} & \text{if } |P| \leq Q \\ v_s |P| + 2M\sqrt{1 - \alpha^2} & \text{if } |P| \geq Q \end{cases}, \end{aligned} \quad (28)$$

where

$$\alpha = \frac{v_s}{v_c}, \quad Q = \frac{2Mv_s}{v_c \sqrt{v_c^2 - v_s^2}}. \quad (29)$$

The behavior is quite similar to what is found for the spectral function¹⁵.

1. Equal velocities $v_s = v_c = v$

For $v_s = v_c = v$ one can obtain the following representation

$$\begin{aligned} \chi_{nn}(\omega, 2k_{F,\sigma} + q) &\approx \frac{\Gamma^2(1-d) Z_1 A'^2}{\pi (2v)^{2d-1}} \int_{-\infty}^{\infty} d\theta \frac{|f_1(2\theta)|^2}{c(\theta)^{2-2d}} \\ &\times \text{Im} F \left(1-d, 1-d, 1, \frac{\omega^2 - v^2 q^2}{c^2(\theta)} \right), \end{aligned} \quad (30)$$

where $c(\theta) = 2M \cosh(\theta)$. The imaginary part of the hypergeometric function vanishes unless $c(\theta) < \sqrt{\omega^2 - v^2 q^2}$. This implies that the response function is nonzero only if $\omega^2 > v^2 q^2 + 4M^2$, in agreement with (28). Just above the threshold ($0 < s/2M \ll 1$) we may use the transformation formulas for hypergeometric functions to obtain ($s^2 = \omega^2 - v^2 q^2$)

$$\begin{aligned} \text{Im} F \left(1-d, 1-d, 1, \frac{s^2}{c^2(\theta)} \right) &= -\frac{\Gamma(1-2d) \sin(\pi 2d)}{\Gamma^2(1-d)} \\ &\times F \left(d, d, 2d, 1 - \frac{s^2}{c^2(\theta)} \right) \left(\frac{s^2}{c^2(\theta)} - 1 \right)^{2d-1} \\ &\times \Theta(s^2 - c^2(\theta)), \end{aligned} \quad (31)$$

where $\Theta(x)$ is the Heaviside function. The remaining θ -integral in (30) is therefore over a very small interval $[-\text{arccosh}(s/2M), \text{arccosh}(s/2M)]$ and can be taken by Taylor-expanding the integrand. The leading contribution to the behavior just above the threshold is

$$\begin{aligned} \chi_{nn}(\omega, 2k_{F,\sigma} + q) &\propto \left(\frac{s - 2M}{M} \right)^{\frac{1}{2} + 2d}, \\ \frac{s - 2M}{M} &\rightarrow 0. \end{aligned} \quad (32)$$

Here we have used that $\beta_c^2 > 1/2$, in which case we have

$$f_1(2\theta) \propto \theta, \quad \text{for } \theta \rightarrow 0. \quad (33)$$

At the Luther-Emery point $\beta_c^2 = \frac{1}{2}^{27}$ there is a different power law increase in (32) (the exponent is $2d - \frac{1}{2}$). As $\beta_c^2 \rightarrow \frac{1}{2}$ from above the region in which (32) holds shrinks to zero. The important result here is that χ_{nn} vanishes as the threshold is approached from above. There are no threshold singularities! The behavior for large frequencies $\omega \gg \sqrt{v^2 q^2 + 4M^2}$ (but necessarily $\omega \ll t$ for field theory to apply) is

$$\chi_{nn}(\omega, 2k_{F,\sigma} + q) \propto s^{2d-2+\beta_c^2}, \quad s \gg M. \quad (34)$$

2. Different velocities $v_s \neq v_c$

In the case of different spin and charge velocities $\frac{v_s}{v_c} \equiv \alpha < 1$ one may represent χ_{nn} as

$$\begin{aligned} \chi_{nn}(\omega, 2k_{F,\sigma} + q) &\approx \frac{Z_1 A'^2}{\Gamma^2(d)(2v_s)^{2d-1}} \\ &\times \int_{-\infty}^{\infty} d\theta_+ d\theta_- |f_1(2\theta_-)|^2 (\Omega\Omega')^{d-1} \Theta(\Omega) \Theta(\Omega'), \end{aligned} \quad (35)$$

where

$$\begin{aligned} \Omega &= \omega - v_s q - 2M \cosh(\theta_-) [\cosh(\theta_+) - \alpha \sinh(\theta_+)], \\ \Omega' &= \omega + v_s q - 2M \cosh(\theta_-) [\cosh(\theta_+) + \alpha \sinh(\theta_+)]. \end{aligned} \quad (36)$$

One easily checks that (35) leads to a threshold described by (28). The remaining integrals in (35) are evaluated numerically.

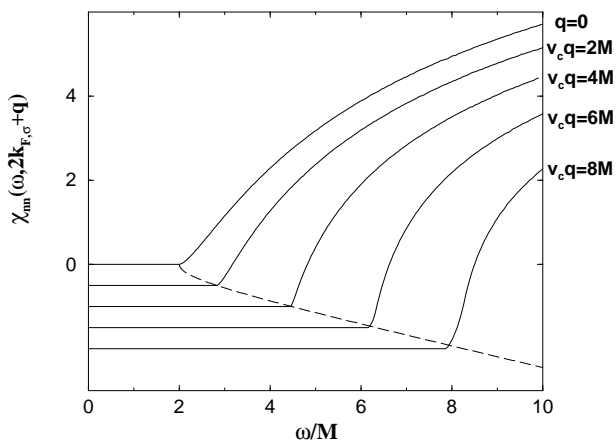


FIG. 2: $\chi_{nn}(\omega, 2k_{F,\sigma} + q)$ for $\beta_c = \beta_s = 1$, $\alpha = 0.851$ and several different values of $v_c q$. The curves have been offset. The dashed line is the threshold when spinons carry zero momentum $\sqrt{4M^2 + v_c^2 q^2}$.

A remarkable feature of the half-filled Mott insulator is the presence of two dispersing features in the

spectral function, that are associated with v_s and v_c respectively^{2,15}. A natural question is whether an analogous feature exists in the density-density response. We have analyzed (35) for several sets of parameters β_c , β_s , α and found that in all cases $\chi_{nn}(\omega, 2k_{F,\sigma} + q)$ is rather featureless. There are no singularities or peaks that can be associated with v_c and v_s separately. We also do not find any threshold singularities as the magnetic field is increased. In Fig. 2 we plot $\chi_{nn}(\omega, 2k_{F,\sigma} + q)$ for $\beta_c = \beta_s = 1$ and $\alpha = 0.851$, which corresponds to the half-filled Hubbard model in zero magnetic field at $U = 1$ ($v_c = 2.15ta_0$, $v_s = 1.83ta_0$). At $\omega \sim 8M$ one can just see that the threshold is below the curve $\sqrt{4M^2 + v_c^2 q^2}$.

IV. EXCITONS: $\beta_c^2 < \frac{1}{2}$

In the regime $\beta_c^2 < \frac{1}{2}$ soliton and antisoliton can form excitonic bound states which for the SGM are known as breathers. There are

$$\mathcal{N} = \left\lceil \frac{1 - \beta^2}{\beta^2} \right\rceil \quad (37)$$

different types of excitons, where $[x]$ denotes the integer part of x . We denote the different excitons by e_1, e_2, \dots . The exciton gaps are given by

$$M_n = 2M \sin(n\pi\xi/2), \quad n = 1, \dots, \mathcal{N}. \quad (38)$$

It follows from the transformation properties under $\Phi_c \rightarrow -\Phi_c$ that only the “odd” excitons e_{2n+1} couple to the density operator. For simplicity we take $\beta_c > 1/2$ from now, in which case we only have to consider the first exciton e_1 . In this regime of β_c the leading contributions of the spectral sum to the dynamical density-density correlator are given by

$$\chi_{nn}(\omega, k) = \chi_{nn}^{\text{exc}}(\omega, k) + \chi_{nn}^{s\bar{s}}(\omega, k), \quad (39)$$

where $\chi_{nn}^{\text{exc}}(\omega, k)$ and $\chi_{nn}^{s\bar{s}}(\omega, k)$ denote the contributions from intermediate states with one exciton and many spinons and one soliton, one antisoliton and many spinons respectively. We have already calculated $\chi_{nn}^{s\bar{s}}(\omega, k)$ above. For small k it is given by (25) and for $k \approx k_{F,\sigma}$ by (35). The exciton contribution can be calculated by the same method¹⁰ and we now present the results.

A. Behavior around $k = 0$

Here the exciton is visible as a sharp δ -function peak at an energy below the soliton-antisoliton scattering continuum

$$\chi_{nn}^{\text{exc}}(\omega, q) = A^2 g_0 \frac{v_c^2 q^2}{\omega} \delta(\omega - \sqrt{v_c^2 q^2 + M_1^2}), \quad (40)$$

where

$$g_0 = \frac{\pi\lambda^2\xi^2}{\sin^2(\pi\xi)},$$

$$\lambda = 2\cos\left(\frac{\pi\xi}{2}\right)\sqrt{2\sin\left(\frac{\pi\xi}{2}\right)}\exp\left(-\int_0^{\pi\xi}\frac{dt}{2\pi\sin t}\right). \quad (41)$$

The result (40) is again related by the equations of motion (26) to the corresponding contribution to the optical conductivity¹⁴. The dynamical density susceptibility, (39), for $v_c q = 0.2M$, is plotted in Fig. 3. For $\beta_c < 1/\sqrt{2}$ the breather contribution (40) appears and the spectral weight is gradually transferred from the soliton-antisoliton continuum to the coherent breather peak.

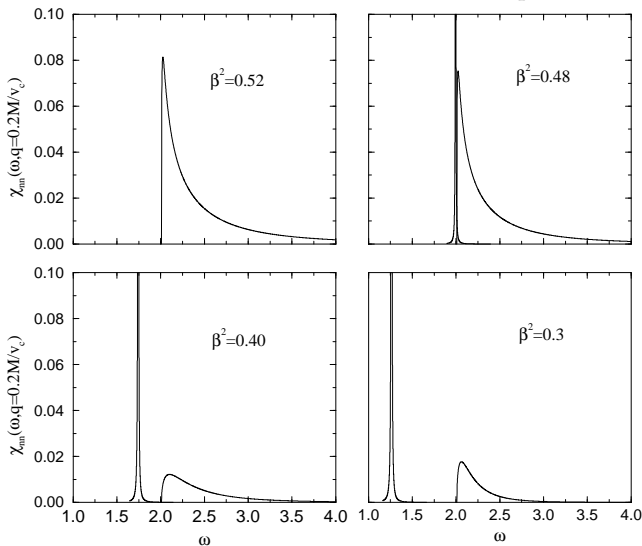


FIG. 3: $\chi_{nn}(\omega, q = 0.2M/v_c)$ for different values of β_c . We have broadened the delta function by convoluting it with a Lorentzian in order to exhibit the transfer of spectral weight from the soliton-antisoliton continuum to the coherent breather peak.

B. Behavior around $q = 2k_{F,\sigma}$

In the vicinity of $q = 2k_{F,\sigma}$ the exciton contributes to the dynamical density-density correlation function via an exciton-spinon scattering continuum with threshold

$$E_{\text{thres}} = \min_q \left[v_s |P - q| + \sqrt{M_1^2 + v_c^2 q^2} \right]$$

$$= \begin{cases} \sqrt{M_1^2 + v_c^2 P^2} & \text{if } |P| \leq Q' \\ v_s |P| + M_1 \sqrt{1 - \alpha^2} & \text{if } |P| \geq Q' \end{cases}, \quad (42)$$

where

$$Q' = \frac{M_1 v_s}{v_c \sqrt{v_c^2 - v_s^2}}. \quad (43)$$

The exciton contribution to the dynamical density-density correlation function is given by

$$\chi_{nn}^{\text{exc}}(\omega, 2k_{F,\sigma} + q) \approx \frac{2\pi Z_1 A'^2}{\Gamma^2(d)(2v_s)^{2d-1}}$$

$$\times \left[\frac{\lambda\xi}{2\cos(\pi\xi/2)} \right]^2 \int_{-\infty}^{\infty} d\theta (\Sigma\Sigma')^{d-1} \Theta(\Sigma) \Theta(\Sigma'), \quad (44)$$

where

$$\Sigma = \omega - v_s q - M_1 [\cosh(\theta) - \alpha \sinh(\theta)],$$

$$\Sigma' = \omega + v_s q - M_1 [\cosh(\theta) + \alpha \sinh(\theta)]. \quad (45)$$

One readily deduces by inspection of equations (45) and (44) that for fixed q the exciton contribution to χ exhibits a cusp at a frequency

$$\omega_{\text{cusp}} = \sqrt{M_1^2 + v_c^2 q^2}. \quad (46)$$

If we fix the momentum transfer to be $q = Q'$, this cusp turns into a singularity. In order to exhibit these interesting features we plot $\chi_{nn}(\omega, 2k_{F,\sigma} + q)$ for $\xi = 0.6$, $\alpha = 0.8$ and different values of q in Fig.4.

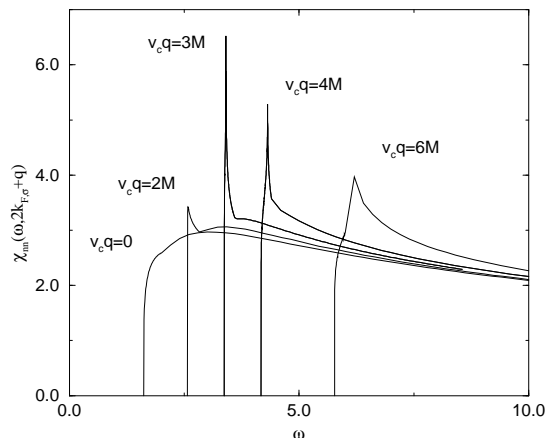


FIG. 4: $\chi_{nn}(\omega, 2k_{F,\sigma} + q)$ for $\alpha = 0.8$, $\beta_s = 1$ and $\xi = 0.6$. For $\omega \approx \omega_{\text{cusp}}$ one can clearly see the cusp due to the breather contribution. As $v_c q$ approaches $v_c Q' \approx 2.157M$ the cusp turns into a singularity.

V. SUMMARY

We have studied the dynamical density-density response of half-filled 1D Mott insulators for the case where the Mott gap is small compared to the hopping matrix element t . We have allowed for the presence of a magnetic field that partially magnetizes the ground state. Unlike

the spectral function, the density-density response function does not exhibit prominent, dispersing features associated with the spin and charge degrees of freedom respectively. Due to the momentum dependence of the matrix elements in the gapped charge sector, $\chi_{nn}(\omega, k)$ tends to zero as the threshold is approached from above: irrespective of the magnitude of the applied magnetic field there are no threshold singularities.

In the parameter region of the extended Hubbard model where excitons are formed, the dynamical density-density response exhibits a *cusp* at some specific value of energy transfer for momentum transfers k close to $2k_{F,\sigma}$.

This cusp turns into a singularity for one particular value of k . These features should be experimentally observable in small-gap quasi-1D Mott insulators.

Acknowledgments

FHLE acknowledges support by the DOE (DE-AC02-98 CH 10886) and the EPSRC (grants AF/100201 and GR/N19359). We thank M. Fabrizio, F. Gebhard and A.A. Nersesyan for discussions.

-
- ¹ N. F. Mott, *Metal-Insulator Transitions*, 2nd ed., Taylor and Francis, London (1990); F. Gebhard, *The Mott Metal-Insulator Transition*, Springer, Berlin (1997).
- ² C. Kim, Z.X. Shen, N. Montoyama, H. Eisaki, S. Uchida, T. Tohyama and S. Maekawa, Phys. Rev. **B56**, 15589 (1997).
- ³ R. Neudert *et al.*, Phys. Rev. Lett. **81**, 657 (1998).
- ⁴ F. Gebhard, K. Bott, M. Scheidler, P. Thomas, and S.W. Koch, Phil. Mag. B **75**, 1, 13, 47 (1997); F.B. Gallagher and S. Mazumdar, Phys. Rev. B. **56**, 15025 (1997).
- ⁵ W. Stephan and K. Penc, Phys. Rev. **B 54**, 17269 (1996); K. Penc and W. Stephan, Phys. Rev. **B 62**, 12707 (2000).
- ⁶ T. Ishiguro and K. Yamaji, *Organic Superconductors*, Springer Verlag, Berlin 1990; C. Bourbonnais and D. Jerome, in “Advances in Synthetic Metals, Twenty years of Progress in Science and Technology”, ed. by P. Bernier, S. Lefrant and G. Bidan (Elsevier, New York, 1999), p. 206-301 and references therein. See also cond-mat - 9903101.
- ⁷ A. Luther, Phys. Rev. **B14**, 2153 (1976); A.B. Zamolodchikov and Al.B. Zamolodchikov, Annals of Physics **120**, 253 (1979); H. Bergknoff and H. Thacker, Phys. Rev. **D19**, 3666 (1979); V.E. Korepin, Theor. Mat. Phys. **41**, 169 (1979).
- ⁸ H. Frahm and V.E. Korepin, Phys. Rev. **B42**, 10553 (1990), *ibid* **B43**, 5653 (1991).
- ⁹ F.H.L. Essler and H. Frahm, Phys.Rev. **B60**, 8540 (1999).
- ¹⁰ F. A. Smirnov, *Form Factors in Completely Integrable Models of Quantum Field Theory*, World Scientific, Singapore (1992); M. Karowski and P. Weisz, Nucl. Phys. **B139**, 455 (1978); H. Babujian, A. Fring, M. Karowski and A. Zapletal, Nucl. Phys. **B538**, 535 (1999); A. Fring, G. Mussardo and P. Simonetti, Nucl.Phys. **B393**, 413 (1993).
- ¹¹ S. Lukyanov, Comm. Math. Phys. **167**, 183 (1995), S. Lukyanov, Mod. Phys. Lett. **A12**, 2911 (1997).
- ¹² E. Jeckelmann, F. Gebhard and F. H. L. Essler, Phys. Rev. Lett. **85**, 3910 (2000).
- ¹³ D. Controzzi, F.H.L. Essler and A.M. Tsvelik, Phys. Rev. Lett. **86** 680 (2001).
- ¹⁴ F.H.L. Essler, F. Gebhard and E. Jeckelmann, Phys. Rev. **B64**, 5119 (2001).
- ¹⁵ F.H.L. Essler and A.M. Tsvelik, Phys. Rev. Lett. **88**, 096403 (2002); Phys. Rev. **B65**, 115117 (2002).
- ¹⁶ T. Fujii and N. Kawakami, J. Phys. Soc. Jpn **68**, 2331 (1999).
- ¹⁷ A. O. Gogolin, A. A. Nersesyan and A. M. Tsvelik, *Bosonization and Strongly Correlated Systems*, Cambridge University Press (1999).
- ¹⁸ O. J. Heilmann and E. H. Lieb, Ann. N.Y. Acad. Sci. **172**, 583 (1971); C. N. Yang, Phys. Rev. Lett. **63**, 2144 (1989).
- ¹⁹ F. Woynarovich, J. Phys. **A22**, 4243 (1989).
- ²⁰ E. Melzer, Nucl. Phys. **443**, 553 (1995); see also F. Woynarovich and P. Forgács, Nucl. Phys. **B 498**, 565 (1997).
- ²¹ F. H. L. Essler and V. E. Korepin, Phys. Rev. Lett. **72**, 908 (1994); Nucl. Phys. **B426**, 505 (1994).
- ²² F. Woynarovich, J. Phys. A **29**, L37 (1996); F. Woynarovich and P. Forgács, Nucl. Phys. **B 538**, 701 (1999).
- ²³ V.J. Emery, in *Highly Conducting One-Dimensional Solids*, eds J.T. Devreese, R.P. Evrard and V.E. van Doren (Plenum, New York, 1979); J.W. Cannon and E. Fradkin, Phys. Rev. **B41**, 9435 (1990); M. Nakamura, Phys. Rev. **B61**, 16377 (2000).
- ²⁴ E. Jeckelmann, unpublished (preprints cond-mat/0204244 and cond-mat/0203500).
- ²⁵ J. Cardy and G. Mussardo, Nucl. Phys. **B410**, 451 (1993).
- ²⁶ The contribution of (13) to χ_{nn} is easily calculated by the formfactor method and is found to be finite for $q \rightarrow 0$ at fixed ω (this is obvious as (13) is a Lorentz scalar and the contribution to the correlation function therefore is a function of $s^2 = \omega^2 - v^2 q^2$). This would imply an infinite optical conductivity by (26), in contradiction to Ref.13.
- ²⁷ A. Luther and V.J. Emery, Phys. Rev. Lett. **33**, 589 (1974).